Original research article

IJAO The International Journal of Artificial Organs

Virtual stenting of intracranial aneurysms: A pilot study for the prediction of treatment success based on hemodynamic simulations

The International Journal of Artificial Organs
1–8

DOI: 10.1177/0391398818775521
journals.sagepub.com/home/jao
SAGE

Philipp Berg[1,2], Sylvia Saalfeld[2,3], Gábor Janiga[1,2], Olivier Brina[4], Nicole M Cancelliere[5], Paolo Machi[4] and Vitor M Pereira[5,6]

Abstract

Endovascular treatment of intracranial aneurysms using flow-diverting devices has revolutionized the treatment of large and complex lesions due to its minimally invasive nature and potential clinical outcomes. However, incomplete or delayed occlusion and persistent intracranial aneurysm growth are still an issue for up to one-third of the patients. We evaluated two patients with intracranial aneurysm located at the internal carotid artery who were treated with flow-diverting devices and had opposite outcomes. Both patients presented with similar aneurysms and were treated with the same device, but after a 1-year follow-up, one case presented with complete occlusion (Case 1) and the other required further treatment (Case 2). To reproduce the interventions, virtual stents were deployed and blood flow simulations were carried out using the respective patient-specific geometries. Afterward, hemodynamic metrics such as aneurysmal inflow reduction, wall shear stresses, oscillatory shear, and inflow concentration indices were quantified. The hemodynamic simulations reveal that for both cases, the neck inflow was clearly reduced due to the therapy (Case 1: 19%, Case 2: 35%). In addition, relevant hemodynamic parameters such as time-averaged wall shear stress (Case 1: 35.6%, Case 2: 57%) and oscillatory shear (Case 1: 33.1%, Case 2: 26.7%) were decreased considerably. However, although stronger relative reductions occurred in the unsuccessful case, the absolute flow values in the successful case were approximately halved. The findings demonstrate that a high relative effect of endovascular devices is not necessarily associated with the desired treatment outcome. Instead, it appears that a successful intracranial aneurysm therapy requires a certain patient-specific inflow threshold.

Keywords

Intracranial aneurysm, flow-diverter, hemodynamics, virtual stenting, computational fluid dynamics

Date received: 1 February 2018; accepted: 16 April 2018

Introduction

Intracranial aneurysms are arterial dilatations of the cerebral vasculature and occur at several locations in the Circle of Willis.[1–3] They are more common in bifurcations, but sidewall aneurysms are particularly located in the internal carotid artery (ICA). Carotid sidewall aneurysms account nearly to 40% of all cases and tend to enlarge and cause compression of cranial nerves or brain structures. Treatment for these lesions has always been a challenge until the advent of the flow-diverting stents (FDSs).[4] While surgical clipping was associated with severe morbidity and perioperative complications, classic endovascular treatment using coils with or without regular intracranial stents was associated with high recurrence rates. FDSs were

[1]Department of Fluid Dynamics and Technical Flows, University of Magdeburg, Magdeburg, Germany
[2]Forschungscampus *STIMULATE*, Magdeburg, Germany
[3]Department of Simulation and Graphics, University of Magdeburg, Magdeburg, Germany
[4]Interventional Neuroradiology Unit, University Hospital of Geneva, Geneva, Switzerland
[5]Joint Department of Medical Imaging, Toronto Western Hospital, University Health Network, Toronto, ON, Canada
[6]Division of Neurosurgery, Department of Surgery, Toronto Western Hospital, University Health Network, Toronto, ON, Canada

Corresponding author:
Philipp Berg, Department of Fluid Dynamics and Technical Flows, University of Magdeburg, Universitaetsplatz 2, Magdeburg 39106, Germany.
Email: berg@ovgu.de

introduced to treat large and giant intracranial aneurysms in the anterior circulation. These show superior results when compared to any other treatment modality.[5–7]

Overall, FDS results are encouraging as they have been associated with up to 75% complete aneurysm occlusion in 1 year and 5% morbimortality.[8–10] Main complications are delayed aneurysm rupture, ischemic lesions as well as delayed parent vessel occlusion.[11] Some basic research using virtual techniques and computational fluid dynamics has been used to assess the results of treatment. A simple approach was proposed by Lee et al.[12] in 2011. The group used a porous medium to reproduce the effect of a densely braided flow-diverter stent. However, the consideration of a two-dimensional, spherical aneurysm model clearly limited this study. Another method was presented by Bock et al.,[13] who used finite element analysis to virtually deploy a neurovascular stent. They were able to compare different stent designs with respect to their aneurysm neck coverage. In addition, Ma et al.[14,15] developed an advanced deployment tool for cerebral aneurysms and demonstrated its reliability using in vitro silicone phantom measurements.[16] However, due to extensive computational resources and enormous simulation times, the method is so far inapplicable in a clinical context.

Cebral et al.[17] used a fast virtual stenting (FVS) technique to identify an intra-aneurysmal pressure increase due to treatment with a flow-diverter. In another study, the same method was applied to investigate side branches jailed by flow-diverters.[18] The authors demonstrated that in rabbit models, perforators remain patent and therefore do not seem to risk therapy-induced side branch occlusion. Furthermore, Xiang et al.[19] virtually investigated the effect of pipeline embolization devices for the endovascular treatment of cerebral aneurysms (possessing completely different shapes and locations) and replicated three clinical therapies. Based on their simulation results, the highest reduction of the aneurysmal average velocity, the aneurysm inflow rate, and the time-averaged wall shear stress (AWSS) were achieved for a case that fully occluded within the first 3 months. The other two cases with late (6 months) or incomplete occlusion suffered from significantly lower flow reduction rates compared to the first. Recently, Bouillot et al.[20] presented an advanced geometrical deployment tool that was validated using contrast-enhanced cone beam computed tomography (CT) and enables a prediction of the stent struts after potential flow-diverter oversizing or undersizing.

Overall, several realistic stenting techniques exist throughout the literature.[21] However, the number of studies in which these techniques are applied to clinically relevant questions is limited.[22–25] The present study addresses the aforementioned concerns and focuses on two clinical aneurysm cases located at identical sites of the ICA. Furthermore, both aneurysms possess a similar phenotype leading to the decision to treat each case using a flow-diverting device. After 3 months, one aneurysm fully occluded, while the other required further treatment. Here, three more stent layers over a 2-year period of time had to be added until a complete thrombosis was obtained. In order to understand the occurring phenomena, the treatment procedure is reproduced using a virtual stenting approach. In addition, three-dimensional hemodynamic simulations are carried out to quantify the efficacy of each intervention. Our results help to improve the understanding of this minimally invasive therapy, thus leading to recommendations toward future clinical procedures.

Methods

Patients and flow-diverter treatment

Two patients harboring an intracranial aneurysm located at the ICA were investigated. For the minimally invasive treatment, pipeline embolization devices (PED; Covidien Neurovascular, Irvine, California, USA) were used. In the first patient (Case 1), a PED 4.5 × 20 mm was chosen leading to complete intra-saccular thrombosis after 3 months. The second patient (Case 2) was treated using a PED 4.0 × 18 mm. Here, the outcome was completely different since occlusion was only possible after the addition of three further flow-diverter layers. Overall, the treatment procedure for Case 2 took approximately 2 years until complete occlusion occurred.

The images used for the three-dimensional (3D) reconstruction of the aneurysm models were obtained from 3D rotational angiogram DICOMs acquired by a Philips Allura angiography system. Image resolution for the cases was 0.207 mm^3. The 3D segmentation was performed using threshold-based segmentation via the XtraVision workstation (Philips Healthcare, Best, The Netherlands). Surface editing and smoothing were performed with AneuFuse (B3C Software, Italy). After the segmentation process, inlets and outlets were truncated at a suitable distance from the aneurysms (see Figure 1, top row). This ensures an appropriate development of the flow structures and reduces the influence of the applied boundary conditions.

Virtual stent deployment

Based on the segmentation results, a FVS method was applied.[26] Here, the identical initial parameters for the PEDs were chosen in order to account for a high-quality reproduction of the interventions (Case 1: PED 4.5 × 20 mm, Case 2: PED 4.0 × 18 mm). In addition to the segmented aneurysm surface models, a vessel centerline was required. For this purpose, the Vascular Modeling Toolkit (VMTK) was used.[27] Since the FVS method is based on the geometric deformation of the stent model, virtual stenting results are generated within seconds on a standard personal computer. As observed in Figure 1 (bottom row), a realistic stenting result, including an appropriate vessel wall apposition and deployment length, was obtained. This is particularly important, since the method considers each individual stent strut

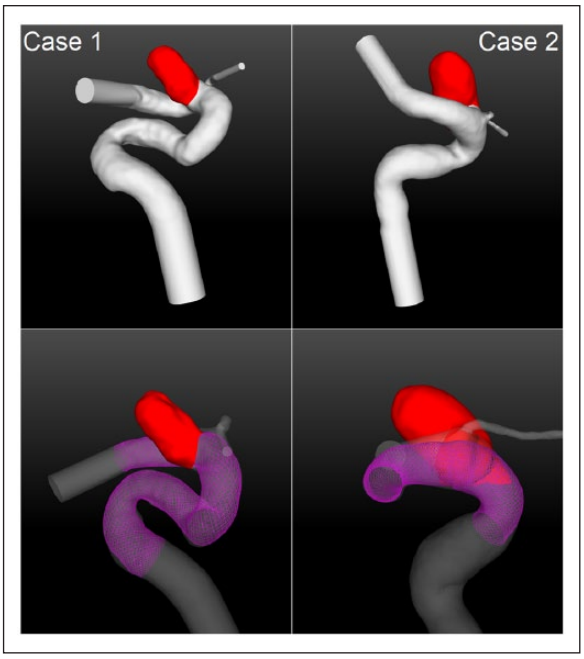

Figure 1. Top row: illustration of the patient-specific aneurysms (red) located at the internal carotid artery. Both aneurysms are situated at almost identical locations and possess a similar phenotype. Bottom row: virtual stent deployment (purple) for both cases using identical flow-diverting devices in the actual clinical treatment (Case 1: PED 4.5 × 20 mm; Case 2: PED 4 × 18 mm).

(diameter $d_{strut} = 33\,\mu m$). Hence, local effects caused by the flow-diverter geometry can be evaluated. It is important to note that the utilized FVS technique was validated with in vivo and in vitro experiments and has been applied to several clinically relevant research topics.[24,25,28] The virtual stenting results for this study were reviewed by an experienced neuroradiologist.

Hemodynamic simulation

To capture the three-dimensional blood flow phenomena that occur before and after the deployment of a flow-diverter, numerical simulations were carried out. In preparation, both domains of interest were spatially discretized using STAR-CCM+11.06 (Siemens Product Lifecycle Management Software Inc., Plano, TX, USA). In order to resolve the existing velocity gradients, prism as well as polyhedral elements were chosen. Here, a global base size of 0.1 mm and a cell size of 0.013 mm for the stent struts were found to be appropriate according to a previous mesh sensitivity analysis.[29] This resulted in the following number of elements (pre/post): Case 1 (3.1 million/8.6 million) and Case 2 (3.3 million/9.1 million), see Supplementary Figure S1 for a visual impression of the discretized cell struts.

After the mesh generation, computational fluid dynamics was used to solve the governing equations for the conservation of mass and momentum. Again, the commercial fluid solver STAR-CCM+ 11.06 was chosen, since it enables a robust simulation environment and is strongly parallelizable. Due to unavailable patient-specific inflow boundary conditions, realistic flow waveforms were adjusted. The time-dependent flow curves were acquired in a healthy volunteer using 7T phase-contrast magnetic resonance imaging.[30] The aneurysm walls as well as the flow-diverters were assumed to be rigid, since no information regarding the actual deformation is available and the pulsatility within the cerebral vasculature is rather small. Flow-splitting was applied at the outlet cross-sections according to the corresponding surface areas. This approach is based on the principle of minimal work (Murray's law) and provides more realistic results compared to the commonly used assumption of a constant zero pressure at the outlets.[31] Blood was treated as an incompressible (with a density of $\rho = 1055\,kg/m^3$) and Newtonian (with a dynamic viscosity of $\eta = 4\,mPa\,s$) fluid and a laminar flow behavior was assumed. A time step size of $\Delta t = 1e{-}3\,s$ was chosen, while for each step residuals of 1e–5 for continuity and all velocity components were requested. In order to obtain a periodic solution, three cardiac cycles (time period $T = 1\,s$) were considered for each simulation. Afterward, the first two cycles were discarded and only the last was included in the post-processing. Overall, a sufficient simulation environment was built to carry out realistic hemodynamic simulations within the cerebral vasculature.

Analysis

To be able to compare the two interventions and their different treatment outcomes, qualitative as well as quantitative analyses of the simulation results were carried out. The impact of a flow-diverting device on the corresponding hemodynamic situation was captured using path lines as well as iso-surface velocities (0.3 m/s). These properties enable a visual impression of the stent-induced blood flow modifications.

Furthermore, relevant hemodynamic metrics on the aneurysm surface were compared, while the focus was laid on AWSS as well as on the oscillatory shear index (OSI). The latter expresses how strongly shear stresses change their direction within one cardiac cycle. Furthermore, important flow values such as the neck inflow rate and the inflow concentration index (ICI)[32] were considered as well.

In addition to the hemodynamic variables, morphological parameters were compared. Here, the aneurysms were analyzed with respect to not only their size (e.g. volume, surface area, aspect ratio[33]), but also to their shape complexity. For this purpose, advanced metrics were chosen, such as the ellipticity index, the non-sphericity index, and the undulation index.[34,35]

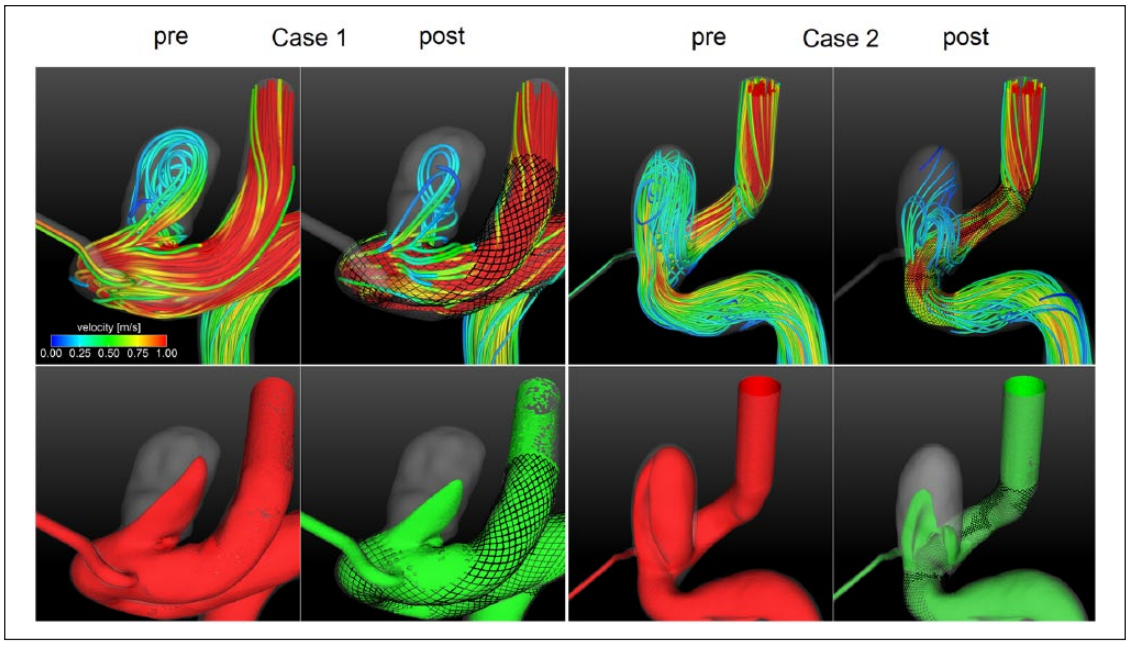

Figure 2. Qualitative results of the hemodynamic simulations pre- and post-virtual flow-diverter placement. Top row: path lines color-coded by velocity magnitude. Bottom row: cycle-averaged iso-surface velocity (0.3 m/s) before (red) and after (green) treatment is used for Case 1 (left) and Case 2 (right). The device-related blood flow reduction into the aneurysms is clearly observed.

Results

Since the hemodynamic simulations provide detailed information regarding the existing flow phenomena, qualitative as well as quantitative results are presented.

Qualitative comparison

The analysis of velocity-encoded path lines demonstrates that in Case 1, nearly no change in the existing flow structure occurs (see Figure 2). Only a slight reduction in the velocity values is visually present, but the existence of a stable vortex remains. In contrast to this observation, Case 2 experiences an impact on the flow situation caused by the addition of a flow-diverter. The course of the path lines changes considerably due to the treatment. In addition, cycle-averaged velocity iso-surfaces based on a threshold value of 0.3 m/s are used for the qualitative description. Again, only slight relative reductions are present in the successfully treated case (Case 1). However, the flow-diverting device in Case 2 leads to a clearly stronger velocity decrease.

In addition to the impression of the velocity field, Figure 3 shows the effect of the flow on the luminal surfaces due to shear stress. The top row illustrates AWSS for both patients before and after treatment. Increased values are mainly present at the parent artery proximal and distal to each aneurysm. Furthermore, the entering inflow jet leads to higher values compared to the rest of the aneurysm sac. However, as observed in both cases, the shape of the flow-diverter leads to a re-direction of the blood, which results in an overall decrease in the AWSS. A similar behavior is observed for the oscillating shear. While different spots of increased OSI exist before the intervention, the placement of the corresponding flow-diverter leads to a visual reduction as well as a changed appearance of the scalar field (see Figure 3, bottom row).

Quantitative comparison

Beside the qualitative comparison of both cases, Figure 4 provides a quantitative analysis of the time-dependent flow parameters. First, the inflow rate into each aneurysm sac was calculated. The presented curves reveal the efficacy of each PED, which leads to a mean decrease of 19% and 35% for Case 1 and Case 2, respectively. Second, the inflow area was measured within the aneurysm ostium and again a decrease of 3.1% and 9.3% (Case 1 and Case 2, respectively) was obtained.

However, it must be noted that the absolute values in Case 1 are clearly lower compared to those in Case 2. Particularly, at every time point of the cardiac cycle, the inflow rate of the first patient was lower before treatment compared to the values after the intervention in Case 2. Hence, a strong relative improvement does not necessarily result in a successful aneurysm occlusion.

To further quantify the investigated aneurysms as well as their hemodynamic environment, Tables 1 and 2 present characteristic morphological and hemodynamic parameters. The comparison of shape values such as aspect ratios,

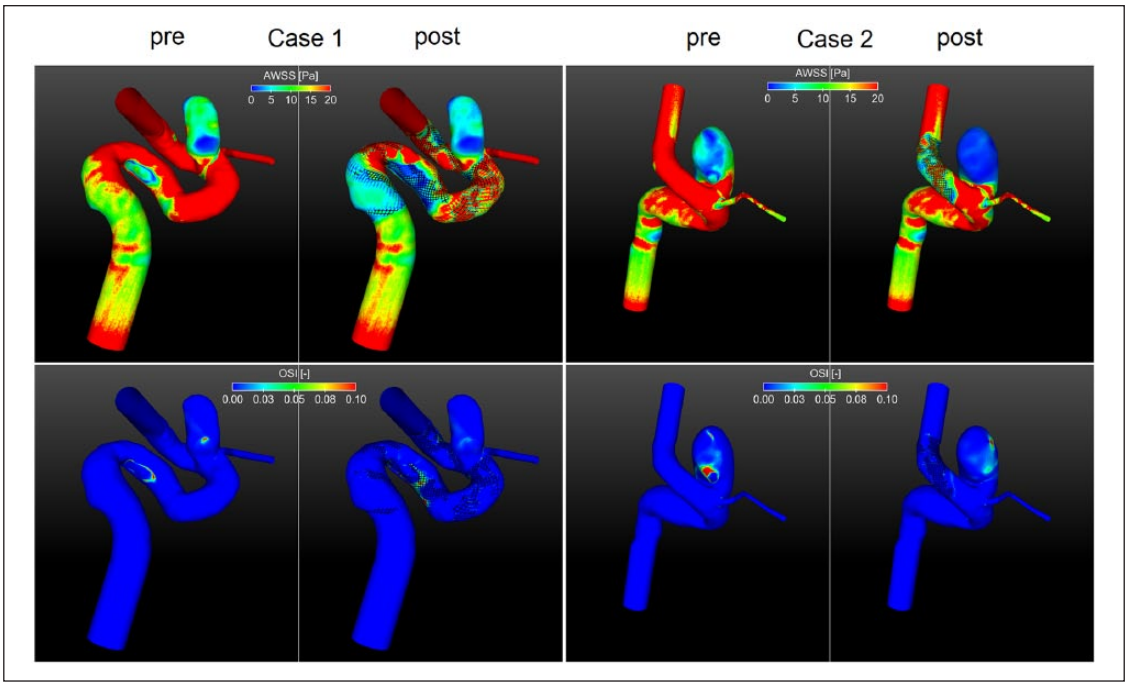

Figure 3. Hemodynamic results on the luminal surface of both aneurysms pre- and post-virtual stent placement. Top row: time-averaged wall shear stress (AWSS); bottom row: oscillatory shear index (OSI). Although the treatment leads to a clear reduction of the shear stresses along the aneurysm wall, increased oscillation can occur due to the effect of flow-diversion (see Table 2).

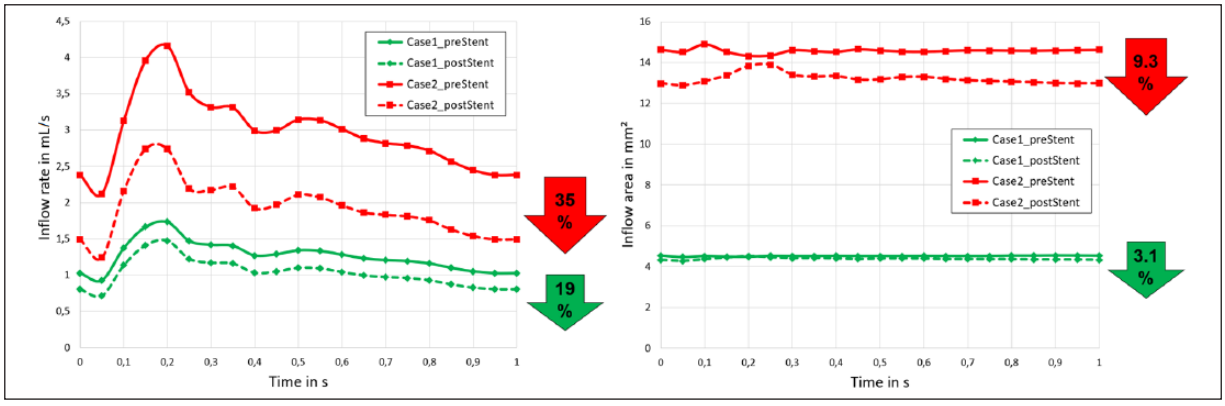

Figure 4. Treatment efficacy for both virtual flow-diverter placements: inflow rate into the aneurysm sac (left) and corresponding inflow area (right). Note that for both parameters, the stent efficacy was higher for the unsuccessful intervention (Case 2). However, although the relative improvement was smaller, the absolute values of the successful case (Case 1) are on a clearly lower plateau.

ellipticity, non-sphericity, and undulation confirms the physician's observation that both cases possess a high similarity aside from their actual location. However, clear differences occur with respect to the actual size. For all considered properties (aneurysm volume, aneurysm surface, aneurysm ostium area), Case 2 possesses clearly larger values compared to Case 1.

An analysis of Table 2 further confirms the findings illustrated in Figure 4. Time- and spatially-averaged wall shear stresses on each aneurysm sac were clearly reduced due to the flow-diverter therapy. Here, a reduction of more than one-third (Case 1) and one-half (Case 2) are achieved. However, regarding the oscillatory shear, an interesting observation can be made: Although the peak values (OSI_{max}) decrease by approximately one-third, the spatially-averaged OSI increases in both cases. Therefore, the implantation of a flow-diverting device not only dampens the flow, but also leads to higher average oscillations. Finally, the analysis of flow parameters such as ICI and Q_{in} again demonstrates that even though Case 2 achieves a

higher efficacy (e.g. a flow reduction of over 30%), absolute values in Case 1 are on a clearly lower plateau.

Discussion

Our pilot study demonstrates the hemodynamic changes after FDS treatment in two ICA aneurysms. They were both located in the paraclinoid segment of the ICA and possessed a similar shape. Both patients were treated using PED flow-diverters, however, experienced entirely opposite outcomes. One aneurysm was completely occluded after 3 months and the second required several extra stent layers up to 2 years after the initial treatment. Unsteady hemodynamic simulations based on pre- and post-treatment scenarios revealed that for Case 2, a higher stent efficacy with respect to inflow reduction was obtained (35%) compared to Case 1 (19%). Furthermore, the analysis of other relevant hemodynamic parameters (e.g. AWSS, OSI, ICI) confirmed that the treatment of Case 2 had a stronger relative effect on the flow situation.

At first, these findings appear to be contradictory to initial expectations, but indeed they enable an improved understanding with respect to flow-diverter therapy of ICA aneurysms: (1) A relative performance of an endovascular treatment does not necessarily lead to a successful intervention. Even though several hemodynamic parameters were clearly reduced, persistence of the aneurysm is still possible. (2) Reaching an absolute inflow threshold, which depends on the type of aneurysm, seems to be required and associated with a complete occlusion result in the short term. Hence, even if the relative improvement appears to be small, it might be sufficient to obtain a successful aneurysm occlusion. However, it clearly needs to pointed out that other metrics such as blood residence time, modified wall shear stress distributions, and also non-flow-related changes might lead to a better therapy outcome.

Since this computational study requires several interdisciplinary working steps, including various assumptions and simplifications, certain limitations exist. First, preprocessing involves potential sources of error. Since it has recently been shown that the choice of the reconstruction kernel can already have a substantial impact on the subsequent geometries and simulations, careful processing of the acquired images is required.[36] Second, the FVS method contains simplifications with respect to reality. Since it is based on geometric deformations, physical interactions that occur both during the opening process and the wall attachment are not taken into account. Nevertheless, the chosen approach is an explicit formulation of the individual stent struts, was validated using in vivo and in vitro experiments, and arbitrary stent diameters, lengths, pore angles and strut sizes can be considered.[26] Furthermore, the stent deployment can be carried out within seconds, which makes the approach clinically applicable. Third, the hemodynamic simulations underlie clear assumptions with respect to boundary conditions as well as the treatment of blood. Although patient-specific flow conditions would be desirable, Valen-Sendstad et al.[37] emphasized the importance of a realistic geometry reconstruction. Even though blood clearly shows a non-Newtonian behavior in vessels of small calibers,[38] various studies demonstrated that considering blood as a Newtonian fluid is reasonable.[39,40] Furthermore, the simulations were performed under identical conditions, which allows for an appropriate relative comparison. Finally, the number of aneurysms considered in this study is small. The identification of similar patient-specific aneurysms with different treatment outcome is

Table 1. Morphological comparison of the considered ICA aneurysms.

Parameter	Case 1	Case 2	Difference
V (mm^3)	57.21	230.32	173.11
A (mm^2)	73.82	183.67	109.85
A_o (mm^2)	7.76	20.25	12.49
AR (–)	1.85	1.61	–0.24
EI (–)	0.276	0.272	–0.004
NSI (–)	0.228	0.215	–0.013
UI (–)	0.075	0.058	–0.017

V: volume; A: aneurysm surface area; A_o: ostium area; AR: aspect ratio; EI: ellipticity index; NSI: non-sphericity index; UI: undulation index; ICA: internal carotid artery.

Table 2. Hemodynamic comparison of the considered ICA aneurysms including the relative reduction due to treatment.

Parameter	Case 1			Case 2		
	Pre	Post	Red. %	Pre	Post	Red. %
$AWSS_{mean}$ (Pa)	12.47	8.03	35.6	8.31	3.57	57
OSI_{mean} (–)	1.8e–3	3.2e–3	–74.3	4.8e–3	5.7e–3	–19.4
OSI_{max} (–)	0.438	0.293	33.1	0.359	0.263	26.7
ICI (–)	0.31	0.26	16.4	0.23	0.16	28.5
A_{in} (mm^2)	4.52	4.38	3.1	14.56	13.21	9.3
Q_{in} (mL/s)	1.26	1.03	18.6	2.96	1.92	35.1

$AWSS_{mean}$: spatially- and time-averaged wall shear stress; OSI_{mean}: mean oscillatory shear index; OSI_{max}: maximum oscillatory shear index; ICI: inflow concentration index; A_{in}: mean aneurysm inflow area; Q_{in}: mean aneurysm inflow rate; ICA: internal carotid artery.

difficult. However, more aneurysms are required to confirm the presented hemodynamic observations.

For future studies, our group intends to improve the above-mentioned limitations. Particularly, more aneurysms will be studied and the measurements of patient-specific flow conditions will be used. Furthermore, if individual, reliable measurements of wall properties (e.g. wall thickness, strength, elasticity) become available, they should clearly be integrated into the simulation setup.[41]

Conclusion

Our pilot study demonstrates that although a better hemodynamic efficiency was obtained in the unsuccessful case, relative improvement does not necessarily lead to better aneurysm occlusion. Hence, it is indicated that a patient-specific absolute flow threshold might be required in order to receive a successful therapy outcome. However, other metrics such as blood residence times or inflow jet modification certainly further influence the treatment result. Therefore, further studies with large cohorts of patients will be required to validate these results and help to identify therapy success measures.

Declaration of conflicting interests

The author(s) declared no potential conflicts of interest with respect to the research, authorship, and/or publication of this article.

Ethical approval

All procedures performed in studies involving human participants were in accordance with the ethical standards of the institutional and/or national research committee and with the 1964 Helsinki Declaration and its later amendments or comparable ethical standards. For this type of study, formal consent is not required.

Funding

The author(s) disclosed receipt of the following financial support for the research, authorship, and/or publication of this article: The work is partly funded by the Federal Ministry of Education and Research in Germany within the Forschungscampus *STIMULATE* under Grant No. 13GW0095A. The work is also funded by the Swiss National Science Foundation grants (Nos SNF 32003B_160222 and SNF 320030_156813).

Informed consent

Informed consent was obtained from all individual participants included in the study.

References

1. Gasparotti R and Liserre R. Intracranial aneurysms. *Eur Radiol* 2005; 15: 441–447.
2. Rinkel GJ, Djibuti M, Algra A, et al. Prevalence and risk of rupture of intracranial aneurysms: a systematic review. *Stroke* 1998; 29: 251–256.
3. Pereira VM, Brina O, Gonzalez AM, et al. Biology and hemodynamics of aneurismal vasculopathies. *Eur J Radiol* 2013; 82: 1606–1617.
4. Pierot L. Flow diverter stents in the treatment of intracranial aneurysms: where are we? *J Neuroradiol* 2011; 38: 40–46.
5. Jevsek M, Mounayer C and Seruga T. Endovascular treatment of unruptured aneurysms of cavernous and ophthalmic segment of internal carotid artery with flow diverter device Pipeline. *Radiol Oncol* 2016; 50: 378–384.
6. Wang A, Santarelli J and Stiefel MF. Pipeline embolization device as primary treatment for cervical internal carotid artery pseudoaneurysms. *Surg Neurol Int* 2017; 8: 3.
7. Pereira VM, Brina O, Delattre BM, et al. Assessment of intra-aneurysmal flow modification after flow diverter stent placement with four-dimensional flow MRI: a feasibility study. *J Neurointerv Surg* 2015; 7: 913–919.
8. Brinjikji W, Lanzino G, Cloft HJ, et al. Risk factors for ischemic complications following pipeline embolization device treatment of intracranial aneurysms: results from the IntrePED study. *AJNR Am J Neuroradiol* 2016; 37: 1673–1678.
9. Brinjikji W, Murad MH, Lanzino G, et al. Endovascular treatment of intracranial aneurysms with flow diverters: a meta-analysis. *Stroke* 2013; 44: 442–447.
10. Kallmes DF, Brinjikji W, Boccardi E, et al. Aneurysm Study of Pipeline in an Observational Registry (ASPIRe). *Interv Neurol* 2016; 5: 89–99.
11. Van Rooij WJ, Sluzewski M and van der Laak C. Flow diverters for unruptured internal carotid artery aneurysms: dangerous and not yet an alternative for conventional endovascular techniques. *AJNR Am J Neuroradiol* 2013; 34: 3–4.
12. Lee CJ, Townsend S and Srinivas K. Optimisation of stents for cerebral aneurysm. In: Kuzmin A (ed.) *Computational fluid dynamics 2010*. Berlin: Springer, 2011, pp. 377–382.
13. Bock DS, Iannaccone F, Santis DG, et al. Our capricious vessels: the influence of stent design and vessel geometry on the mechanics of intracranial aneurysm stent deployment. *J Biomech* 2012; 45: 1353–1359.
14. Ma D, Dumont TM, Kosukegawa H, et al. High fidelity virtual stenting (HiFiVS) for intracranial aneurysm flow diversion: in vitro and in silico. *Ann Biomed Eng* 2013; 41: 2143–2156.
15. Ma D, Xiang J, Choi H, et al. Enhanced aneurysmal flow diversion using a dynamic push-pull technique: an experimental and modeling study. *AJNR Am J Neuroradiol* 2014; 35: 1779–1785.
16. Zhang Q, Meng Z, Zhang Y, et al. Phantom-based experimental validation of fast virtual deployment of self-expandable stents for cerebral aneurysms. *Biomed Eng Online* 2016; 15: 125.
17. Cebral JR, Mut F, Raschi M, et al. Aneurysm rupture following treatment with flow-diverting stents: computational hemodynamics analysis of treatment. *AJNR Am J Neuroradiol* 2011; 32: 27–33.
18. Cebral JR, Raschi M, Mut F, et al. Analysis of flow changes in side branches jailed by flow diverters in rabbit models. *Int J Numer Method Biomed Eng* 2014; 30: 988–999.
19. Xiang J, Damiano RJ, Lin N, et al. High-fidelity virtual stenting: modeling of flow diverter deployment for hemody-

namic characterization of complex intracranial aneurysms. *J Neurosurg* 2015; 123: 832–840.
20. Bouillot P, Brina O, Ouared R, et al. Geometrical deployment for braided stent. *Med Image Anal* 2016; 30: 85–94.
21. Berg P, Daróczy L and Janiga G. Virtual stenting for intracranial aneurysms. In: Balocco S, Zuluaga MA, Zahnd G, et al. (eds) *Computing and visualization for intravascular imaging and computer-assisted stenting*, Elsevier, 2017, pp. 371–411.
22. Berg P, Iosif C, Ponsonnard S, et al. Endothelialization of over- and undersized flow-diverter stents at covered vessel side branches: an in vivo and in silico study. *J Biomech* 2016; 49: 4–12.
23. Bouillot P, Brina O, Yilmaz H, et al. Virtual-versus-real implantation of flow diverters: clinical potential and influence of vascular geometry. *AJNR Am J Neuroradiol*. Epub ahead of print 30 June 2016. DOI: 10.3174/ajnr.A4845
24. Iosif C, Berg P, Ponsonnard S, et al. Role of terminal and anastomotic circulation in the patency of arteries jailed by flow-diverting stents: animal flow model evaluation and preliminary results. *J Neurosurg* 2016; 125: 898–908.
25. Iosif C, Berg P, Ponsonnard S, et al. Role of terminal and anastomotic circulation in the patency of arteries jailed by flow-diverting stents: from hemodynamic changes to ostia surface modifications. *J Neurosurg* 2017; 126: 1702–1713.
26. Janiga G, Rössl C, Skalej M, et al. Realistic virtual intracranial stenting and computational fluid dynamics for treatment analysis. *J Biomech* 2013; 46: 7–12.
27. Antiga L, Piccinelli M, Botti L, et al. An image-based modeling framework for patient-specific computational hemodynamics. *Med Biol Eng Comput* 2008; 46: 1097–1112.
28. Sindeev S, Arnold PG, Frolov S, et al. Phase-contrast MRI versus numerical simulation to quantify hemodynamical changes in cerebral aneurysms after flow diverter treatment. *PLoS One* 2018; 13: e0190696.
29. Janiga G, Berg P, Beuing O, et al. Recommendations for accurate numerical blood flow simulations of stented intracranial aneurysms. *Biomed Tech (Berl)* 2013; 58: 303–314.
30. Berg P, Stucht D, Janiga G, et al. Cerebral blood flow in a healthy Circle of Willis and two intracranial aneurysms: computational fluid dynamics versus four-dimensional phase-contrast magnetic resonance imaging. *J Biomech Eng* 2014; 136. DOI: 10.1115/1.4026108
31. Chnafa C, Brina O, Pereira VM, et al. Better than nothing: a rational approach for minimizing the impact of outflow strategy on cerebrovascular simulations. *AJNR Am J Neuroradiol* 2018; 39: 337–343.
32. Xiang J, Tutino VM, Snyder KV, et al. CFD: computational fluid dynamics or confounding factor dissemination? The role of hemodynamics in intracranial aneurysm rupture risk assessment. *AJNR Am J Neuroradiol* 2014; 35: 1849–1857.
33. Weir B, Amidei C, Kongable G, et al. The aspect ratio (dome/neck) of ruptured and unruptured aneurysms. *J Neurosurg* 2003; 99: 447–451.
34. Dhar S, Tremmel M, Mocco J, et al. Morphology parameters for intracranial aneurysm rupture risk assessment. *Neurosurgery* 2008; 63: 185–197.
35. Xiang J, Natarajan SK, Tremmel M, et al. Hemodynamic-morphologic discriminants for intracranial aneurysm rupture. *Stroke* 2011; 42: 144–152.
36. Berg P, Saalfeld S, Voß S, et al. Does the DSA reconstruction kernel affect hemodynamic predictions in intracranial aneurysms? An analysis of geometry and blood flow variations. *J Neurointerv Surg* 2018; 10: 290–296.
37. Valen-Sendstad K, Piccinelli M, KrishnankuttyRema R, et al. Estimation of inlet flow rates for image-based aneurysm CFD models: where and how to begin? *Ann Biomed Eng* 2015; 43: 1422–1431.
38. Carty G, Chatpun S and Espino DM. Modeling blood flow through intracranial aneurysms: a comparison of Newtonian and non-Newtonian viscosity. *J Med Biol Eng* 2016; 36: 396–409.
39. Fisher C and Rossmann JS. Effect of non-Newtonian behavior on hemodynamics of cerebral aneurysms. *J Biomech Eng* 2009; 131: 091004.
40. Morales HG, Larrabide I, Geers AJ, et al. Newtonian and non-Newtonian blood flow in coiled cerebral aneurysms. *J Biomech* 2013; 46: 2158–2164.
41. Voß S, Glaßer S, Hoffmann T, et al. Fluid-structure simulations of a ruptured intracranial aneurysm: constant versus patient-specific wall thickness. *Comput Math Methods Med* 2016; 2016: 9854539.